Received 13 April 2022; revised 12 May 2022; accepted 18 June 2022. Date of publication 23 June 2022; date of current version 12 July 2022.
The review of this article was arranged by Editor P. Pavan.

Digital Object Identifier 10.1109/JEDS.2022.3185618

Comprehensive Design and Numerical Study of GaN Vertical MPS Diodes Towards Alleviated Electric Field Crowding and Efficient Carrier Injection

HENG WANG [1,2], SIHAO CHEN [1,2], HANG CHEN [1,2], AND CHAO LIU [1,2]

1 School of Microelectronics, Institute of Novel Semiconductors, Shandong Technology Center of Nanodevices and Integration, State Key Laboratory of Crystal Materials, Shandong University, Jinan 250100, China
2 Shenzhen Research Institute, Shandong University, Shenzhen 518057, China

CORRESPONDING AUTHOR: C. LIU (e-mail: chao.liu@sdu.edu.cn)

This work was supported in part by the National Natural Science Foundation of China under Grant 62104135; in part by the Shenzhen Science and Technology Program under Grant JCYJ20210324141212030; in part by the Guangdong Basic and Applied Basic Research Foundation under Grant 2020A1515111018; in part by the Shandong Provincial Natural Science Foundation under Grant ZR2020QF079; and in part by the Qilu Young Scholar Program under Grant 11500089963075.

ABSTRACT In this paper, we systematically investigate the impact of the key structural parameters on the reverse and forward characteristics of gallium nitride (GaN) based vertical merged pn-Schottky (MPS) diode by numerical simulation. In comparison with conventional GaN-based vertical Schottky barrier diode, the MPS structure can suppress the high electric field at the Schottky interface with the inserted p-GaN, thereby enhancing the reverse breakdown characteristics. However, the adoption of the p-GaN structure can result in a locally crowded electric field at reserve bias condition and thus a premature breakdown of the device. Moreover, the p-GaN structure depletes the vertical channel region, which may degrade the on-performance at forward bias condition. We found that the doping concentration, width, and depth of the p-GaN structure are closely correlated with the electric field distribution at reverse bias and the channel resistance at forward bias, and thus determines the reverse and forward characteristics of the MPS diodes. The unique forward unipolar/bipolar characteristics of the MPS diode was also investigated and discussed systematically. The results can pave the way for the development of GaN power electronic devices towards a compact high-frequency and high-voltage power electronic system.

INDEX TERMS Breakdown voltage, device optimization, gallium nitride (GaN), specific ON-resistance, vertical merged pn-Schottky (MPS) diode.

I. INTRODUCTION

In recent years, gallium nitride (GaN) has exhibited tremendous potential for power electronic devices owing to its wider energy band gap, higher breakdown electric field, and higher carrier mobility [1]–[4]. Thanks to the availability of low-dislocation-density bulk GaN substrates and the intrinsic advantages of the vertical device topology, GaN-based vertical SBDs have been developed extensively towards high voltage and high current applications [5]–[7]. However, similar to the lateral GaN SBDs based on the AlGaN/GaN heterostructures, GaN vertical SBDs also suffer from reverse leakage issues due to the energy barrier lowering effect at high reverse bias condition. To achieve a decent device performance, several device architectures have been developed, such as junction barrier Schottky (JBS) diode [8], MPS diode [9]–[12], and trench metal-insulator-semiconductor barrier Schottky (TMBS) diode [13], [14], which are designed to move the peak electric field from the interface of the Schottky junction to the inside of the device at high reverse bias, leading to a higher breakdown voltage and a lower reverse leakage current.

Specially, unlike conventional planar SBDs, MPS diodes combine Schottky contact and Ohmic contact monolithically,

This work is licensed under a Creative Commons Attribution 4.0 License. For more information, see https://creativecommons.org/licenses/by/4.0/

offering SBD-like on-state and switching characteristics, and pn diode-like off-state characteristics. Compared with SBDs, MPS diodes can exhibit bipolar operation mode at forward bias, lower reverse leakage current, and higher reverse breakdown voltage by reducing the electric field at the interface of the Schottky junction. Besides, benefited from the Ohmic contact on the p-GaN region, MPS diodes can demonstrate avalanche and surge capabilities, which are of great significance for their practical applications in power circuits and systems [15]–[17].

The concept of MPS diode was firstly demonstrated and discussed in Si-based devices [18], [19]. Then it was investigated and developed in SiC-based devices [16], [17], [20]–[27]. Niwa *et al.* researched on the forward hybrid unipolar/bipolar operation mode systematically and the "snapback" phenomenon was also investigated and analyzed [25]. Park *et al.* analyzed the physical mechanism behind the high forward pn-junction turn-on voltage in 4H-SiC MPS diode, revealing that the turn-on voltage is closely correlated with the potential difference between the Schottky junction and the pn junction within a MPS diode [26]. Recently, Liu *et al.* experimentally verified the high surge current robustness in GaN vertical pn diodes and their significantly smaller reverse recovery as compared to SiC diodes, which makes GaN MPS diodes particularly attractive for fast switching applications [15]. While GaN-based MPS diodes have been successfully fabricated with breakdown voltage up to 2 kV [9]–[11], the impact of the key design parameters as well as the working principles of GaN-based MPS diodes still remain to be explored systematically. Zhang *et al.* investigated the impact of the lateral dimension of the Schottky regions on the device performance by assuming a fixed p-GaN thickness of 800 nm and p-doping concentration of 2×10^{17} cm^{-3} [12]. However, during practical fabrication process, the p-GaN thickness and doping concentration may vary from the proposed values, which can result in a disparate impact from the lateral dimension. Therefore, the ideal approach is to study the influence of three key design parameters altogether and comprehensively for the purpose of fulfilling a complete design strategy.

In this paper, we systematically studied and analyzed the influence of the key design parameters on the reverse and forward characteristics by varying the doping concentration, width, and thickness of the p-GaN structure by simulation. The relationship between the design parameters and the key device specifications are studied comprehensively, including the breakdown voltage, specific on-resistance, turn-on voltage, forward voltage drop, and pn junction trigger voltage of the GaN-based MPS diodes. The physical mechanism and the analytical models are explored and established for the purpose of explaining the variation trends with different design parameters. We believe that the results in this work can provide sufficient guidance towards the design and fabrication of high performance GaN MPS diodes.

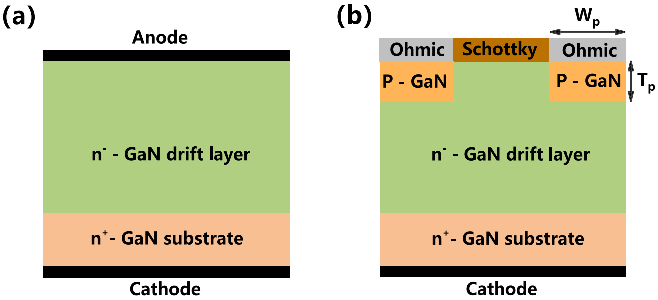

FIGURE 1. The schematic cross section of (a) a conventional GaN-based planar SBD and (b) a GaN-based vertical merged pn-Schottky (MPS) diode.

TABLE 1. Basic device parameters of the simulated model.

Parameters	Value
Schottky barrier height	0.98 eV
Metal work function	5.18 eV
Electron mobility	1158 cm^2/ V·s
Hole mobility	14.97 cm^2/ V·s
Thickness of the drift layer	15 μm
Drift layer doping	2×10^{16} cm^{-3}
Thickness of the substrate	2 μm
Substrate doping	5×10^{18} cm^{-3}
Width of the device cell	10 μm

II. DEVICE ARCHITECTURES AND PRINCIPLES

Fig. 1(a)–(b) show the schematic structure of a conventional planar SBD and a MPS diode. Detailed parameters of the devices are listed in Table 1. The following parameters were varied in order to study their impacts on the MPS device performance: p-doping concentration, p-GaN structure width (W_p), p-GaN structure thickness (T_p). In the MPS diodes, the contact to the p-GaN structure is set to be Ohmic contact, and the contact type to the middle n⁻-GaN drift layer is Schottky contact.

As has been reported, the relatively low breakdown voltage value of the conventional planar SBD is mainly caused by the large reverse leakage current at the Schottky junction, which is determined by the barrier lowering effect under the condition of excessive electric field strength at the Schottky interface. The barrier lowering effect can be attributed to the mirror force and tunneling effect, by which the reduction of the barrier can be expressed by equation (1) [28]:

$$q\Delta\phi = \left[\frac{q^3 E_m}{4\pi\varepsilon_s}\right]^{\frac{1}{2}} = 2qE_m x_m \tag{1}$$

$$E_m = \left[\frac{2qN_D}{\varepsilon_s}(V_{bi}+V_R)\right]^{\frac{1}{2}} \tag{2}$$

where q is the electron charge, N_D is the donor concentration, ε_s represents the semiconductor permittivity, V_{bi} is the built-in potential of Schottky barrier junction, x_m represents the location of the barrier lowering, E_m represents the peak electric field value, and V_R is the external reverse bias.

Thus, to simplify the calculation, assuming that if the thickness is smaller than the critical barrier thickness x_c, the carriers can completely tunnel through the Schottky barrier, so the reduction of the barrier by mirror force and tunneling can be expressed respectively as:

$$q\Delta\phi_{mirror\ force} = \left[\frac{q^7 N_D}{8\pi^2\varepsilon_s^3}(V_{bi}+V_R)\right]^{\frac{1}{4}} \tag{3}$$

$$q\Delta\phi_{tunneling} = x_c\left[\frac{8q^3 N_D}{\varepsilon_s}(V_{bi}+V_R)\right]^{\frac{1}{2}} \tag{4}$$

Specifically, conventional planar SBDs feature a triangular electric field profile along the drift layer, exhibiting a peak electric field located at the Schottky interface. A high E_m attributes to a large V_R, thus causing an obvious barrier lowering effect, resulting in an unideal reverse leakage and breakdown characteristics. By adopting the MPS structure, the depletion effect of p-GaN/n$^-$-GaN junction moves the peak electric field from the Schottky interface into the bulk of the device, which can effectively reduce the electric field at the Schottky interface, alleviating the barrier lowering effect under high electric field, and reducing the reverse leakage current across the Schottky junction. Meanwhile, the increased electric field at the pn junction interface can also result in a reverse leakage current, which is much smaller than that across the Schottky barrier region, due to the absence of the mirror force effect in the pn junction. As a result, the adoption of the MPS structure can effectively reduce the reverse leakage current and avoid the premature breakdown of conventional planar SBDs.

In the following content, the influence of the key structural design parameters on the reverse and forward characteristics of the MPS diodes, as well as the physical mechanism are systematically investigated and analyzed, by using Advanced Physical Models of Semiconductor Devices (APSYS) software [29]. The key physical models used in the simulation include models for carrier drift-diffusion, generation-recombination, continuity and Poisson equations, impact ionization, and electron tunneling. Specifically, the device breakdown process is induced by the joint effect of the tunneling induced leakage and the impact ionization. In the drift-diffusion model, the impact ionization rate is usually expressed using the impact-ionization coefficients α_n and α_p, which can be calculated by the following Chynoweth's Equations (5) and (6) [30], [31]:

$$\alpha_n = 2.9\times10^8\ cm^{-1}\ \times\ e^{\left(\frac{-3.4\ \times\ 10^7\ V/cm}{E}\right)} \tag{5}$$

$$\alpha_p = 1.34\times10^8\ cm^{-1}\ \times\ e^{\left(\frac{-2.03\ \times\ 10^7\ V/cm}{E}\right)} \tag{6}$$

where E is defined as the electric field magnitude in the drift layer. The two coefficients describe the number of electron-hole pairs generated per unit distance traveled by a solitary carrier between two collisions. The physical models and parameters used in our simulation were calibrated with an experimentally fabricated GaN vertical SBD from [32]. The simulated breakdown voltage fits the experimental results well, indicating that the models and key parameters used in our simulation are technologically reasonable.

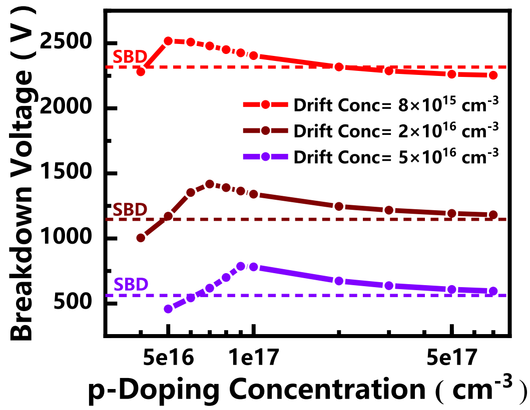

FIGURE 2. Breakdown voltage as a function of the p-doping concentration for the MPS diodes with $T_p = 2.0$ µm, $W_p = 4.5$ µm at a Drift Conc = 8×10^{15} cm^{-3} (red solid line), 2×10^{16} cm^{-3} (Burgundy solid line), and 5×10^{16} cm^{-3} (purple solid line). The three dash lines correspond to the breakdown voltage of the planar SBD at the respective drift concentration.

III. RESULT AND DISCUSSION

A. REVERSE CHARACTERISTICS

In order to fully study the effects of the MPS diode key design parameters, we first discussed the influence of the p-doping concentration on the reverse characteristics, under different background doping concentrations of the n$^-$-GaN drift layer, as shown in Fig. 2. In this case, T_p and W_p are set as 2.0 μm and 4.5 μm, respectively. Note that in this paper, we define the voltage when the reverse current density reaches 1 A/cm^2 as the breakdown voltage. By taking the reverse breakdown voltage of the conventional planar SBD as a reference, we can observe a significant improvement in the breakdown voltage of the MPS diodes. Similar phenomenon is recorded with increased p-doping concentration at different background doping concentrations. The reverse breakdown voltage for the MPS diodes with different background doping concentrations all shows a trend of first increasing and then decreasing as the p-doping concentration increases. With a background doping concentration of 2×10^{16} cm^{-3}, a reverse breakdown voltage of 1418 V can be achieved in the MPS diodes, which is 23.6% higher than that of conventional planar SBDs. Note that a higher p-doping concentration is required to obtain the peak breakdown voltage for the MPS diodes with a higher background doping concentration, which can be attributed to the different total charge depletion effect. Moreover, at a low p-doping concentration ($< 5\times10^{16}$ cm^{-3}), the breakdown voltage of the MPS diodes is lower than that of conventional planar SBDs, due to insufficient electric field shielding effect by the p-GaN structure.

Please note that the p-doping concentration in this work refers to the ionizable acceptor concentration instead of the Mg dopant concentration. Therefore, the investigated range (4×10^{16} cm$^{-3}\sim$ 7×10^{17} cm^{-3}) is much smaller than the

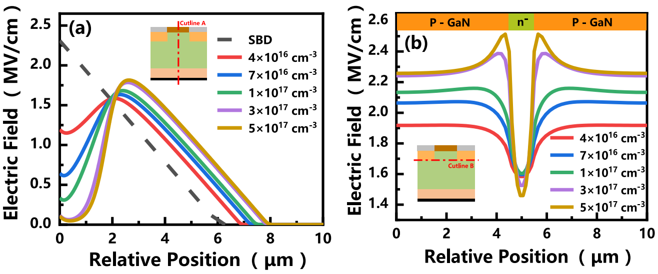

FIGURE 3. Electric field profiles along (a) the midline and (b) the bottom of the p-GaN structure of the MPS diodes with T_p = 2.0 μm, W_p = 4.5 μm with different p-doping concentrations at the reverse bias of 700 V.

Mg dopant concentration typically adopted in experimental devices (10^{18} cm^{-3}~ 10^{19} cm^{-3}), due to the existence of the Mg-H complex compounds formed during the epitaxial process. Moreover, the effect of the electric field on the acceptor ionization is also considered in our simulation. As a result, the acceptor concentration is not equal to the hole concentration, unless the electric field is strong enough to fully ionize the acceptors under the reverse depletion condition.

Fig. 3(a) plots the vertical electric field profiles along the midline of the MPS diodes. It is shown that the electric field at the Schottky interface can be suppressed by the p-GaN structure in the MPS diodes, as compared to the triangular electric field profile shown by the dash line. By increasing the p-doping concentration from 4×10^{16} cm^{-3} to 3×10^{17} cm^{-3}, the electric field shielding effect by the p-GaN can be obviously enhanced, leading to a dramatic reduction in the electric field value at the Schottky interface, which can explain the boosted breakdown voltage with increased p-doping concentration in Fig. 2. Further increasing the p-doping concentration to 5×10^{17} cm^{-3} encounters a saturation in the shielding effect and the electric field value cannot be further reduced at the Schottky interface. In the meantime, an electric field peak occurred in the bulk drift region at a position of about 3 μm from the Schottky interface, which can be correlated with the electric field crowding effect in the vicinity of the p-GaN edges.

To further explore the electric field crowding effect related to the p-GaN structure, we extracted the lateral electric field profiles from the bottom of the p-GaN structure, as show in Fig. 3(b). Note that the electric field at the bottom of the p-GaN is larger than that at the channel region, as a result of the depletion effect by the p-GaN/n$^-$-GaN junction. An increase in the electric field value can be observed with increased p-doping level. As the p-doping concentration increases to above 3×10^{17} cm^{-3}, a locally excessive electrical field occurred at the corner of p-GaN structure, which can result in the premature breakdown of the device. Based on the analysis above, an optimal p-doping concentration of 7×10^{16} cm^{-3} can result in an enhanced electric field shielding effect at the Schottky interface, without an obvious electric field crowding at the corner of the p-GaN structures, leading to a peak breakdown voltage of 1418 V in the MPS diode.

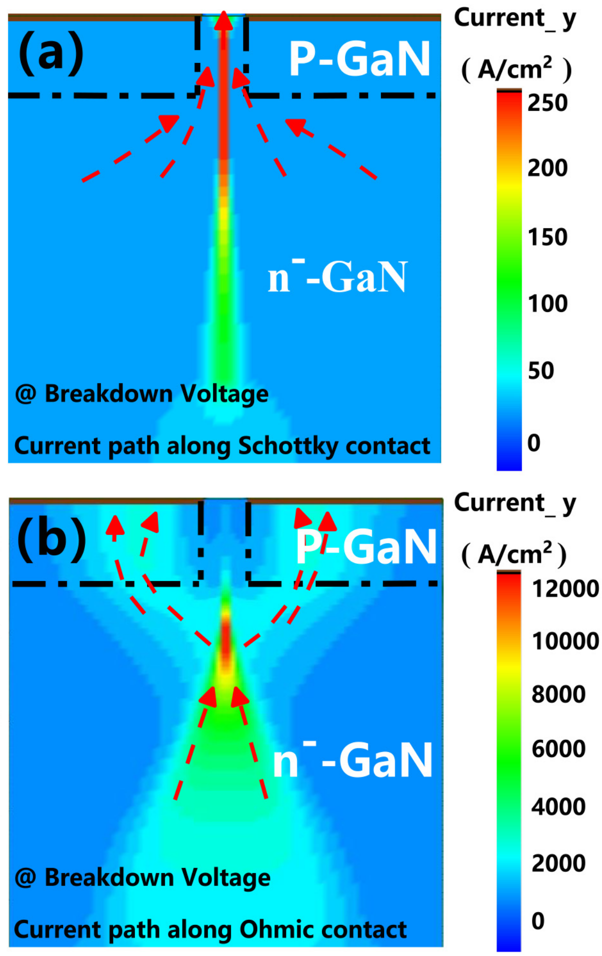

FIGURE 4. Two-dimensional current diagram in the vertical direction with T_p = 2.0 μm, W_p = 4.5 μm, and p-doping concentration of (a) 4×10^{16} cm^{-3}, (b) 7×10^{16} cm^{-3} at breakdown voltage.

As is known, the MPS diodes consist of the Schottky and pn junction regions, which is accompanied two potential leakage paths, either across the Schottky barrier or through the reverse biased pn junction. As a result, the leakage mechanism of the MPS diodes remains to be investigated. Fig. 4 illustrates the two-dimensional current diagram of the MPS diodes with a p-doping concentration of 4×10^{16} cm^{-3} and 7×10^{16} cm^{-3}, respectively. With a low p-doping level of 4×10^{16} cm^{-3} in Fig. 4(a), the reverse leakage current at the breakdown voltage flows through the channel region at the center across the Schottky barrier, indicating insufficient electric field shielding effect by the p-GaN structure. By increasing the p-doping to 7×10^{16} cm^{-3} in Fig. 4(b), an effective electric field shielding effect can be formed, thus eliminating the leakage path across the Schottky region. In the meantime, the reverse leakage current flows through the reverse biased pn junction to the Ohmic contact on the p-GaN structure, which has been observed in experimentally fabricated vertical GaN Fin-JFETs [33], [34]. As a result, by optimizing the p-doping concentration, the reverse breakdown and leakage behavior of the MPS diodes can

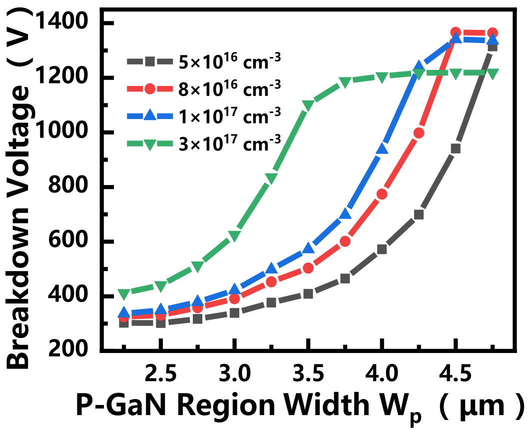

FIGURE 5. **Breakdown voltage as a function of W_p for the MPS diodes with $T_p = 1.5$ μm at p-doping concentration of 5×10^{16} cm^{-3} (black solid line), 8×10^{16} cm^{-3} (red solid line), 1×10^{17} cm^{-3} (blue solid line), and 3×10^{17} cm^{-3} (green solid line).**

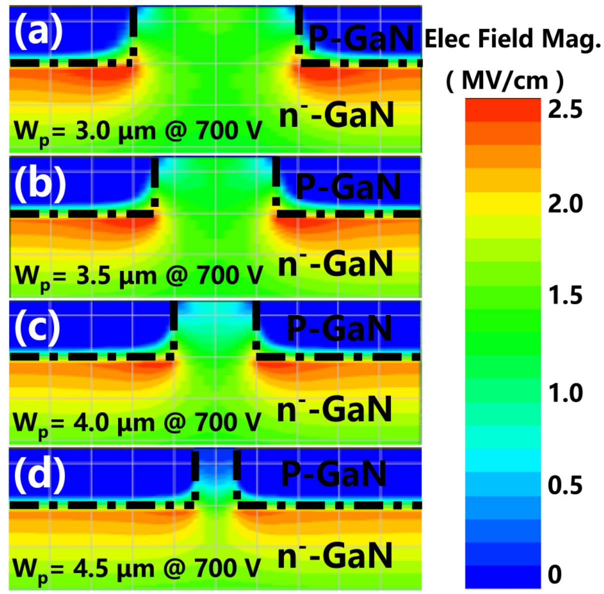

FIGURE 6. **Two-dimensional electric field distribution of the MPS diodes with $T_p = 1.5$ μm, p-doping concentration of 1×10^{17} cm^{-3} and W_p = (a) 3.0 μm, (b) 3.5 μm, (c) 4.0 μm, (d) 4.5 μm at a reverse bias of 700 V.**

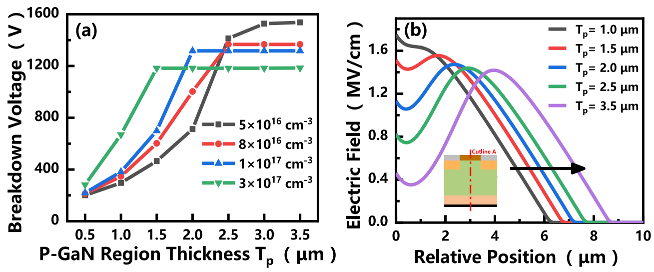

FIGURE 7. **(a) Breakdown voltage as a function of T_p for the MPS diodes with $W_p = 4.0$ μm at a p-doping concentration of 5×10^{16} cm^{-3} (black solid line), 8×10^{16} cm^{-3} (red solid line), 1×10^{17} cm^{-3} (blue solid line), and 3×10^{17} cm^{-3} (green solid line). (b) Electric field profiles along the midline of the MPS diodes with $W_p = 4.0$ μm and p-doping concentration of 8×10^{16} cm^{-3} at different T_p when the reverse bias is 700 V.**

be equivalent to that of a pn diode instead of a conventional planar SBD, leading to a dramatic improvement in the reverse characteristics.

In addition to the p-doping concentration, the geometrical shape of the MPS structure is also closely associated with the breakdown and leakage performance of the MPS diodes. Therefore, we first investigate the influence of the p-GaN width on the breakdown characterizes of the devices, as shown in Fig. 5. The breakdown voltage of the MPS diodes is positively correlated with W_p at all listed p-doping concentrations. For a low p-doping concentration of 5×10^{16} cm^{-3}, the reverse breakdown voltage increases monotonously in the whole range of W_p from 2.25 μm to 4.75 μm. Further increasing p-doping concentration to 8×10^{16} cm^{-3} and above leads to a saturation in the breakdown voltage at a certain W_p. Moreover, with a larger p-doping concentration, a smaller saturation point of W_p can be observed.

For the purpose of analyzing and explaining the trend above, we intercepted the two-dimensional electric field distribution of the MPS diodes at a reverse bias of 700 V, as shown in Fig. 6. The p-GaN width varies from 3.0 μm to 4.5 μm, while the p-GaN thickness is kept as 1.5 μm. The p-GaN structure is marked by the dashed box in the figure. With a small W_p of 3.0 μm, the peak electric field is concentrated at the corner of the p-GaN structure, resulting in a premature breakdown of the device. A more uniform distribution of the electric field underneath the p-type GaN can be observed with increased W_p to 4.5 μm, thanks to the spreading effect of the electric field along the lateral orientation, which well explains the monotonous increase of the breakdown voltage with W_p in Fig. 5. As W_p increases, the electric field at the Schottky interface gradually reduces until an excellent electric field shielding effect is formed in Fig. 6(d). The reduced electric field at the Schottky interface can lead to reduced leakage current at reverse bias condition. Taking all the factors into account, we can conclude that a relatively larger W_p value can produce a stronger electric field shielding effect, thus suppressing the reverse leakage and preventing the premature breakdown of the device.

We then look into how the p-GaN thickness affects the reverse characteristics of the MPS diodes. Fig. 7(a) shows the breakdown voltage as a function of T_p for MPS diodes at different p-doping concentrations. Similar phenomenon can be observed for the MPS diodes with different p-doping concentrations, in which a larger T_p is favorable for enhanced breakdown voltage of the device before the saturation point. Note that the breakdown voltage features a positive relationship with the p-doping concentration at a small T_p, while a lower p-doping concentration is preferred for a decent breakdown voltage in the large T_p range, indicating that there remains an optimum range for the total charges introduced by the p-GaN structure that offers the best electric field shielding effect and breakdown characteristics in the MPS diodes.

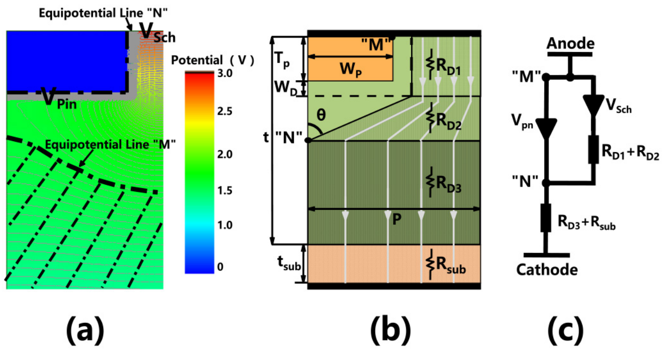

FIGURE 8. (a) Electrostatic potential distribution inside the MPS diode at low injection. (b) Schematic illustration of the current flow in the MPS analytical resistance model. (c) The simplified equivalent circuit gives an intuitive interpretation of the functional components of a MPS diode.

As previously discussed, the electric field at the Schottky interface is directly related to the electric field shielding effect by the p-GaN structure in the MPS diodes. Therefore, we extracted the vertical electric field profiles along the dashed line shown in the inset of Fig. 7(b). As the value of T_p increases, the electric field shielding effect on the Schottky interface is enhanced, resulting in reduced electric field at the Schottky interface. Meanwhile, the peak of the electric field moves into the bulk of the drift layer and the two-dimensional depletion depth is increased, which also contributes to the improved breakdown voltage of the devices.

B. FORWARD CHARACTERISTICS

We have explored the influence of the key design parameters (p-doping concentration, p-GaN width, and p-GaN thickness) on the breakdown voltage of the MPS diodes and clarified the physical mechanism behind the reverse characteristics. Next, we will analyze the effect of the geometrical structural parameters on the forward characteristics. For the purpose to reveal the correlation mechanism between the forward voltage drop (V_F), the pn junction trigger voltage (V_{turn}), the specific ON-resistance at low injection (R_{on1}), the specific ON-resistance at high injection (R_{on2}) and the geometrical structure parameters, we established an analytical resistance model based on the extracted electrostatic potential distribution within the MPS diode, as well as a relevant simplified equivalent circuit, as shown in Fig. 8 [16], [21], [25]. Specifically, Point M and N in Fig. 8(b) corresponds to the equipotential line M and N in Fig. 8(a), where the potential difference between line M and N (V_{MN}) is regarded as the voltage drop on the pn junction.

In the case of low injection, the device resistance R_{on1} can be modeled in series with the channel resistance (R_{D1}), the spread resistance (R_{D2}), the drift layer resistance (R_{D3}), and the substrate resistance (R_{sub}), as shown in Fig. 8(b), which can be expressed by equations (7) to (11):

$$R_{D1} = \rho_D \frac{T_P + W_D}{Z \cdot (P - W_P - W_D)} \tag{7}$$

$$R_{D2} = \frac{\rho_D}{Z \cdot \tan\theta} \ln\left(\frac{P}{P - W_P - W_D}\right) \tag{8}$$

$$R_{D3} = \rho_D \frac{(t - T_P - W_D)\tan\theta - (W_P + W_D)}{P \cdot Z \cdot \tan\theta} \tag{9}$$

$$R_{sub} = \rho_{sub} \frac{t_{sub}}{P \cdot Z} \tag{10}$$

$$R_{on1} = R_{D1} + R_{D2} + R_{D3} + R_{sub} \tag{11}$$

where ρ_D is the resistivity of the drift layer, ρ_{sub} is the resistivity of the substrate, W_D is the depletion width of the pn junction, P is the width of the whole device, t is the thickness of the drift layer, t_{sub} is the thickness of the substrate, and Z is the width in the third dimension of the MPS diode.

The forward voltage drop (V_F) at low current density J_F can be calculated by equations (12) and (13):

$$V_F = V_{Sch} + R_{on1} \cdot J_F \tag{12}$$

$$V_{Sch} = \Phi_B + \frac{kT}{q} \ln\left(\frac{J_F}{AT^2}\right) \tag{13}$$

where Φ_B is the Schottky barrier height, k is the Boltzmann constant, T is the Kelvin temperature, q is the electron charge, and A is the effective Richardson's constant. And V_{Sch} represents the voltage drop across the Schottky barrier.

While in the case of high injection, the high concentration of free carriers injected from the pn junction will lead to a conductance modulation effect and reduce the resistance of the drift region. Therefore, R_{on2} of the MPS diode typically features a much smaller value compared to that of R_{on1}. Moreover, under forward conduction conditions, the on-resistance of the pn diode is much smaller compared to the resistance from the bulk material. Hence, R_{on2} can be roughly simplified into the sum of R_{D3} and R_{sub}.

To better interpret the forward operation mode, the simplified equivalent circuit is symbolled in Fig. 8(c), in which the Schottky barrier diode together with R_{D1} and R_{D2} are connected in parallel with a pn diode at the equipotential point N, then connected in series with R_{D3} and R_{sub}. Under the condition of low injection, the pn junction is in the off state and the MPS diodes work in unipolar operation mode. As long as V_{MN} exceeds the turn on voltage of the pn junction (V_{pn}), the pn junction turns on and the carrier behavior satisfies the high injection condition, thus the MPS diodes switch to bipolar operation mode. Therefore, the pn junction trigger voltage (V_{turn}) can be expressed by equation (14):

$$\begin{aligned} V_{turn} &= \frac{V_{pn} - V_{Sch}}{R_{D1} + R_{D2}} \cdot R_{on1} + V_{Sch} \\ &= \frac{V_{pn} - V_{Sch}}{R_{D1} + R_{D2}} \cdot (R_{D3} + R_{sub}) + V_{pn} \end{aligned} \tag{14}$$

where V_{turn} can be expressed as the sum of V_{pn} and the voltage drop on the resistance R_{D3} and R_{sub}. For a certain GaN-based MPS diode, V_{pn} remains to be around 3 V and R_{sub} is always constant.

As vertical GaN devices are being developed for multi-kilovolt applications, it is of great significance to discuss the applicability of the revealed design trade-offs for higher voltage ratings. Vertical devices with higher breakdown voltage are typically designed with a larger thickness and smaller

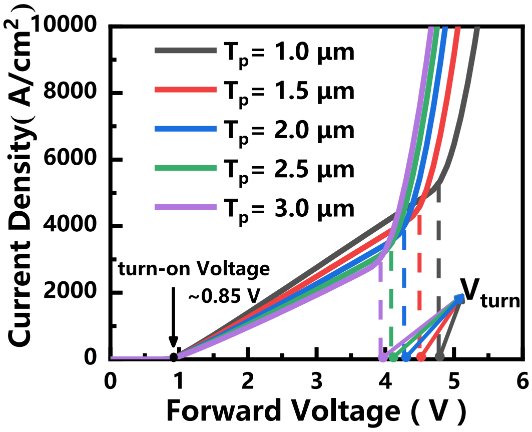

FIGURE 9. Forward I-V characteristics of the MPS diodes with varied p-GaN thickness T_p at W_p of 4.0 μm and p-doping concentration of 1×10^{17} cm^{-3}.

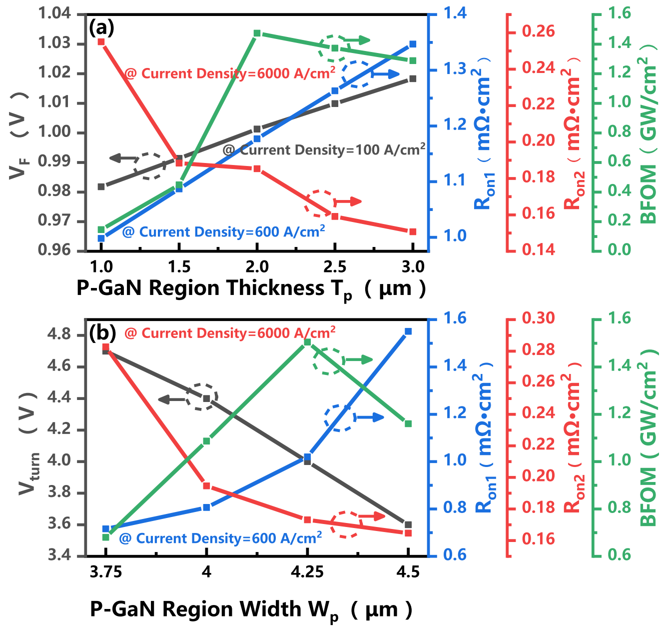

FIGURE 10. (a) The extracted forward voltage drop V_F, specific ON-resistance R_{on1}, R_{on2} and the calculated BFOM as a function of T_p of MPS diodes in on state with $W_p = 4.0$ μm and p-doping concentration of 1×10^{17} cm^{-3} . (b)The pn junction trigger voltage V_{turn}, the specific ON-resistance R_{on1}, R_{on2}, and the calculated BFOM as a function of W_p of the MPS diodes in on state with $T_p = 1.5$ μm and p-doping concentration of 1×10^{17} cm^{-3} .

doping concentration in the drift layer [35], [36], which results in a larger R_{D3} and thus an increased V_{turn}. Consequently, the higher V_{turn} prevents the devices from operating in bipolar mode during forward conduction, which deprives the devices of their surge capability, to the detriment of the practical circuit applications [37]. In order to avoid this, a thicker p-GaN structure is desired, so that the value of R_{D1} and R_{D2} can be increased accordingly due to the enhanced depletion effect from the pn junction. Correspondingly, the V_{turn} of the MPS diodes can be reduced to assure a prompt unipolar/bipolar transition.

To verify the analytical resistance model above, we investigated the influence of the p-GaN thickness T_p on the forward I-V characteristics of the MPS diodes, as is shown in Fig. 9. The MPS diodes turn on to unipolar operation mode at approximately 0.85 V. And at voltages higher than V_{turn}, the diodes switch to bipolar operation mode, showing steeper I-V curves. As T_p increases, the value of V_{turn} reduces monotonically, as the result of reduced $R_{D3,}$ which agrees with (9) and (14).

The forward voltage drop (V_F) and specific ON-resistance as a function of T_p extracted from the I-V curve is plotted in Fig.10(a). It is shown that at low injection region, the value of R_{on1} is increased with T_p, contributing to an increased V_F, while under high injection conditions, R_{on2} decreases with T_p. The increased value of R_{on1} is a combined effect of R_{D1} and R_{D3}, which can be calculated from (7) and (9), respectively. As the channel region is narrower than the drift region, the prolonged current path through the channel region will lead to increased overall resistance with increased T_p. Under high injection conditions, the carriers flow through the pn junction into the drift region. The overall resistance of the MPS diodes decreases with T_p due to the reduced drift region thickness.

In addition, to evaluate the forward and revere characteristics of the GaN MPS diodes simultaneously, the Baliga's Figure of Merit (BFOM) is shown in Fig. 10(a) and calculated by equation (15):

$$BFOM = \frac{BV^2}{R_{on1}} \tag{15}$$

A maximum BFOM value of 1.474 GW/cm^2 can be obtained with a T_p of 2.0 μm, indicating an optimal comprehensive performance of the devices by taking the trade-off issues into consideration.

Fig. 10(b) shows the relationship between V_{turn}, R_{on1}, R_{on2} and W_p. A similar trend of the forward characteristics can be observed with the p-GaN width, in which V_{turn} and R_{on2} decreases with W_p while R_{on1} increases with W_p. For low injection conditions, a larger value of W_p will generate a narrower current channel, exacerbating the current crowding effect and therefore resulting in a larger R_{on1}. A larger W_p will lead to an increased slope of the equipotential line "N" in Fig. 8 (a) and thus a reduced R_{D3}. As a result, the V_{turn} and R_{on2} of the MPS diodes will reduce correspondingly. Furthermore, the BFOM has a maximum value of 1.505 GW/cm^2 when W_p is 4.25 μm.

IV. CONCLUSION

To summarize, we systematically investigated the influence of the key design parameters on the reverse and forward characteristics of GaN-based MPS diodes. By taking advantage of the electric field shielding effect, the electric field at the Schottky junction region of the conventional planar Schottky barrier diodes can be effectively alleviated and the barrier lowering effect at high electric field can be suppressed. In the meantime, an optimal set of parameters is crucial for avoiding the premature breakdown at the corner of the p-GaN structure due to the electric field crowding effect. Based on the on-state I-V characteristics of the MPS diodes, the physical mechanism and the analytical model of the forward conduction are also explored and analyzed. We believe that the findings in this article can provide a theoretical guideline for the design of high-voltage, high-power, and low-loss GaN-based MPS diodes towards the future application in high-efficiency GaN-based power systems.

ACKNOWLEDGMENT

The authors would like to thank J. Yin, and X. Liu for their valuable discussion and technical support.

REFERENCES

[1] M. Xiao, Y. Ma, K. Liu, K. Cheng, and Y. Zhang, "10 kV, 39 mΩ·cm2 multi-channel AlGaN/GaN Schottky barrier diodes," *IEEE Electron Device Lett.*, vol. 42, no. 6, pp. 808–811, Jun. 2021, doi: 10.1109/LED.2021.3076802.

[2] M. Xiao *et al.*, "5 kV multi-channel AlGaN/GaN power Schottky barrier diodes with junction-fin-anode," in *Proc. IEDM*, Dec. 2020, pp. 541–544, doi: 10.1109/IEDM13553.2020.9372025.

[3] C. Liu, R. A. Khadar, and E. Matioli, "GaN-on-Si quasi-vertical power MOSFETs," *IEEE Electron Device Lett.*, vol. 39, no. 1, pp. 71–74, Jan. 2018, doi: 10.1109/LED.2017.2779445.

[4] H. Fu, K. Fu, S. Chowdhury, T. Palacios, and Y. Zhao, "Vertical GaN power devices: Device principles and fabrication technologies—Part II," *IEEE Trans. Power Electron.*, vol. 68, no. 7, pp. 3212–3222, Jul. 2021, doi: 10.1109/TED.2021.3083209.

[5] Y. Cao, R. Chu, R. Li, M. Chen, R. Chang, and B. Hughes, "High-voltage vertical GaN Schottky diode enabled by low-carbon metal-organic chemical vapor deposition growth," *Appl. Phys. Lett.*, vol. 108, no. 6, pp. 1–5, Feb. 2016, doi: 10.1063/1.4941814.

[6] H. Fu, X. Huang, H. Chen, Z. Lu, I. Baranowski, and Y. Zhao, "Ultra-low turn-on voltage and on-resistance vertical GaN-on-GaN Schottky power diodes with high mobility double drift layers," *Appl. Phys. Lett.*, vol. 111, no. 15, pp. 1–5, Oct. 2017, doi: 10.1063/1.4993201.

[7] C. Liu, R. A. Khadar, and E. Matioli, "Vertical GaN-on-Si MOSFETs with monolithically integrated freewheeling Schottky barrier diodes," *IEEE Electron Device Lett.*, vol. 39, no. 7, pp. 1034–1037, Jul. 2018, doi: 10.1109/LED.2018.2841959.

[8] Y. Zhang *et al.*, "Vertical GaN junction barrier Schottky rectifiers by selective ion implantation," *IEEE Electron Device Lett.*, vol. 38, no. 8, pp. 1097–1100, Aug. 2017, doi: 10.1109/LED.2017.2720689.

[9] W. Li *et al.*, "Design and realization of GaN trench junction-barrier-Schottky-diodes," *IEEE Trans. Electron Devices*, vol. 64, no. 4, pp. 1635–1641, Apr. 2017, doi: 10.1109/TED.2017.2662702.

[10] Y. Irokawa *et al.*, "Si^+ ion implanted MPS bulk GaN diodes," *Solid-State Electron.*, vol. 48, no. 5, pp. 827–830, May 2004, doi: 10.1016/j.sse.2003.09.018.

[11] T. Hayashida, T. Nanjo, A. Furukawa, and M. Yamamuka, "Vertical GaN merged PiN Schottky diode with a breakdown voltage of 2 kV," *Appl. Phys. Exp.*, vol. 10, no. 6, pp. 1–3, Jun. 2017, doi: 10.7567/APEX.10.061003.

[12] Y. Zhang, X. Lu, and X. Zou, "Device design assessment of GaN merged P-i-N Schottky diodes," *Electronics*, vol. 8, no. 12, pp. 1–11, Dec. 2019, doi: 10.3390/electronics8121550.

[13] S. Chen, H. Chen, Y. Qiu, and C. Liu, "Systematic design and parametric analysis of GaN vertical trench MOS barrier Schottky diode with p-GaN shielding rings," *IEEE Trans. Electron Devices*, vol. 68, no. 11, pp. 5707–5713, Nov. 2021, doi: 10.1109/TED.2021.3109845.

[14] Y. Zhang *et al.*, "Novel GaN trench MIS barrier Schottky rectifiers with implanted field rings," in *Proc. IEDM*, Dec. 2017, pp. 1–4, doi: 10.1109/IEDM.2016.7838386.

[15] J. Liu *et al.*, "Surge current and avalanche ruggedness of 1.2-kV vertical GaN p-n diodes," *IEEE Trans. Power Electron.*, vol. 36, no. 10, pp. 10959–10964, Oct. 2021, doi: 10.1109/TPEL.2021.3067019.

[16] Y. Huang, T. Erlbacher, J. Buettner, and G. Wachutka, "A trade-off between nominal forward current density and surge current capability for 4.5kV SiC MPS diodes," in *Proc. ISPSD*, Jun. 2016, pp. 63–66, doi: 10.1109/ISPSD.2016.7520778.

[17] L. Liu *et al.*, "Investigation of avalanche capability of 1200V 4H-SiC MPS diodes and JBS diodes," in *Proc. ISPSD*, Sep. 2020, pp. 210–213, doi: 10.1109/ISPSD46842.2020.9170067.

[18] B. M. Wilamowski, "Schottky diodes with high breakdown voltages," *Solid-State Electron.*, vol. 26, no. 5, pp. 491–493, May 1983, doi: 10.1016/0038-1101(83)90106-5.

[19] B. J. Baliga, "Analysis of a high-voltage merged p-i-n/Schottky (MPS) rectifier," *IEEE Electron Device Lett.*, vol. EDL-8, no. 9, pp. 407–409, Sep. 1987, doi: 10.1109/EDL.1987.26676.

[20] V. d'Alessandro *et al.*, "Influence of layout geometries on the behavior of 4H-SiC 600V merged PiN Schottky (MPS) rectifiers," in *Proc. ISPSD*, Jun. 2006, pp. 1–4, doi: 10.1109/ISPSD.2006.1666097.

[21] J. Wu, N. Ren, and K. Sheng, "Design and experimental study of 1.2kV 4H-SiC merged PiN Schottky diode," in *Proc. ISPSD*, May 2019, pp. 203–206, doi: 10.1109/ISPSD.2019.8757619.

[22] Q. Du and X. Tao, "The on-resistance model of silicon carbide merged PiN Schottky (MPS) diodes," in *Proc. IOP Conf. Ser. Mater. Sci. Eng.*, vol. 677, Oct. 2019, pp. 1–14, doi: 10.1088/1757-899X/677/5/052100.

[23] H. Jian-Hua *et al.*, "Simulation study of a mixed terminal structure for 4H-SiC merged PiN/Schottky diode," *Chin. Phys. B*, vol. 20, no. 11, pp. 1–4, Nov. 2011, doi: 10.1088/1674-1056/20/11/118401.

[24] Y. Jiang, W. Sung, J. Baliga, S. Wang, B. Lee, and A. Huang, "Electrical characteristics of 10-kV 4H-SiC MPS rectifiers with high Schottky barrier height," *J. Electron. Mater.*, vol. 27, no. 2, pp. 927–931, Feb. 2018, doi: 10.1007/s11664-017-5812-2.

[25] H. Niwa, J. Suda, and T. Kimoto, "Ultrahigh-voltage SiC MPS diodes with hybrid unipolar/bipolar operation," *IEEE Trans. Electron Devices*, vol. 64, no. 3, pp. 874–881, Mar. 2017, doi: 10.1109/TED.2016.2636573.

[26] J. Park *et al.*, "Control of pn-junction turn-on voltage in 4H-SiC merged PiN Schottky diode," *Appl. Phys. Lett.*, vol. 110, no. 14, pp. 1–5, Apr. 2017, doi: 10.1063/1.4979790.

[27] J. Wu, N. Ren, Q. Guo, and K. Sheng, "A comparative study of silicon carbide merged PiN Schottky diodes with electrical-thermal coupled considerations," *Materials*, vol. 13, no. 11, pp. 1–19, Jun. 2020, doi: 10.3390/ma13112669.

[28] S. M. Sze and K. K. Ng, *Physics of Semiconductor Devices*, 3rd ed. Hoboken, NJ, USA: Wiley, 2007, ch. 3, pp. 147–148.

[29] (Crosslight Softw. Inc., Burnaby, BC, Canada). *APSYS 2018 and APSYS Technical Manuals*. (2018). [Online]. Available: http://www.crosslight.com

[30] A. G. Chynoweth, "Ionization rates for electrons and holes in silicon," *Phys. Rev.*, vol. 109, no. 5, pp. 1537–1540, Mar. 1958, doi: 10.1103/PhysRev.109.1537.

[31] V. K. Sundaramoorthy and I. Nistor, "Study of edge termination structures for high power GaN Schottky diodes," *Physica Status Solidi*, vol. 8, nos. 7–8, pp. 2270–2272, Jul. 2011, doi: 10.1002/pssc.201001032.

[32] X. Jia *et al.*, "Design strategies for mesa-type GaN-based Schottky barrier diodes for obtaining high breakdown voltage and low leakage current," *IEEE Trans. Electron Devices*, vol. 67, no. 5, pp. 1931–1938, May 2020, doi: 10.1109/TED.2020.2978007.

[33] J. Liu *et al.*, "1.2-kV vertical GaN Fin-JFETs: High-temperature characteristics and avalanche capability," *IEEE Trans. Electron Devices*, vol. 68, no. 4, pp. 2025–2032, Apr. 2021, doi: 10.1109/TED.2021.3059192.

[34] J. Liu *et al.*, "1.2 kV Vertical GaN Fin JFETs with robust avalanche and fast switching capabilities," in *Proc. IEDM*, Dec. 2020, pp. 1–4, doi: 10.1109/IEDM13553.2020.9372048.

[35] H. Ohta, N. Asai, F. Horikiri, Y. Narita, T. Yoshida, and T. Mishima, "4.9 kV breakdown voltage vertical GaN p–n junction diodes with high avalanche capability," *Jpn. J. Appl. Phys.*, vol. 36, pp. 1–4, Jun. 2019, doi: 10.7567/1347-4065/ab0cfa.

[36] M. Xiao, R. Zhang, G. Schlenvogt, T. Jokinen, H. Wang, and Y. Zhang, "Vertical GaN superjunction FinFET: A novel device enabling multi-kilovolt and megahertz power switching," in *Proc. DRC*, Jun. 2019, pp. 161–162, doi: 10.1109/DRC46940.2019.9046481.

[37] R. Zhang, X. Lin, J. Liu, S. Mocevic, D. Dong, and Y. Zhang, "Third quadrant conduction loss of 1.2–10 kV SiC MOSFETs: Impact of gate bias control," *IEEE Trans. Power Electron.*, vol. 36, no. 2, pp. 2033–2043, Feb. 2021, doi: 10.1109/TPEL.2020.3006075.